

# Effect of Lattice Coherency on Solution Energies of Impurities: Stability of an Epitaxial InAs Monolayer Deposited on GaAs

著者	Vannarat S., Sluiter Marcel H. F., Kawazoe Yoshiyuki
journal or publication title	Materials Transactions, JIM
volume	40
number	11
page range	1295-1300
year	1999
URL	<a href="http://hdl.handle.net/10097/52212">http://hdl.handle.net/10097/52212</a>

# Effect of Lattice Coherency on Solution Energies of Impurities: Stability of an Epitaxial InAs Monolayer Deposited on GaAs

S. Vannarat, Marcel H. F. Sluiter and Yoshiyuki Kawazoe

*Institute for Materials Research, Tohoku University, Sendai, 980-8577 Japan*

The formation enthalpy of the  $\text{In}_{\text{Ga}}$  defect in GaAs was calculated *ab initio* by a hybrid method consisting of an atomistic- and a continuum calculation. The atomic relaxation of the lattice near the defect was treated with an atomistic calculation, whereas the long-ranged elastic strain energy was obtained from a linear elastic continuum calculation. The solubility of InAs in GaAs at room temperature and the maximum temperature of the miscibility gap in the solid solution phase were determined from the defect formation enthalpy. The results are in good agreement with a thermodynamic assessment. The effect of lattice coherency on the  $c/a$  ratio of epitaxial InAs monolayers grown on (100) GaAs substrates is determined. The stability of such InAs layers with respect to the Ga-rich  $\text{In}_x\text{Ga}_{1-x}\text{As}$  solid solution is predicted.

(Received May 21, 1999; In Final Form July 16, 1999)

**Keywords:** indium arsenide, gallium arsenide, formation energy, defect, heterostructure, *ab-initio* calculation, solubility

## I. Introduction

The growth of InAs on GaAs substrates is known to be of Stranski-Krastanov(SK) type, in which initially 2D monolayers form. When a critical thickness has been reached, the coherency strain induces the growth to switch into 3D mode, where coherent islands form<sup>(1)</sup>. The island formation is believed to be an alternative strain relaxation mechanism<sup>(2)(3)</sup> to the misfit dislocation mechanism. Being an interesting candidate for high quality quantum dots for quantum devices, these islands have inspired detailed studies of InAs/GaAs heterostructures.

One of the interesting phenomena is the atomic diffusion between the islands and the substrate<sup>(4)</sup>. Diffusion will affect the compositions of the materials inside and outside the quantum dots and thus their morphology and other properties. In this work we investigated the stability of thin epitaxial InAs layers (in the early stage of the growth) for the case of a (100) interface plane by considering the possibility of alloying or diffusion of atoms across the interface. The two possibilities are the diffusion of an In atom into the GaAs substrate and the diffusion of a Ga atom from the substrate into the epitaxial layer. However, because of the presence of the nearby InAs/GaAs interface and surface, the latter cannot be evaluated without explicit consideration of the morphology. Consequently, the resulting Ga defect formation enthalpy in this system is a function of many variables. In contrast, the diffusion of In atom into the substrate will form a defect with a well defined thermodynamic property, provided that it is at some distance from the InAs/GaAs interface. As the energy of an In atom dissolved in GaAs is lowest if it substitutes for a Ga atom, we considered that diffusion causes  $\text{In}_{\text{Ga}}$  substitu-

tional defects in the GaAs substrate. Therefore, the formation energy of the  $\text{In}_{\text{Ga}}$  substitutional defect corresponds to the solution energy of InAs into GaAs. This solution energy was computed as a function of the strain condition of the epitaxial InAs layer.

It is known that the epitaxial InAs layers are coherent with the GaAs substrate. The lattice parameter in the interface plane between InAs and GaAs varies as the thickness of the InAs film increases. However, it is reasonable to assume that at the thickness of few monolayers, the epitaxial InAs will take the GaAs lattice parameter in the interface plane. While in-plane the lattice parameter is fixed by the coherency requirement, the perpendicular lattice parameter takes a value that minimizes the energy. By calculating both the formation energy of the  $\text{In}_{\text{Ga}}$  defect and the effect of the strain on the energy of the InAs layer, we can predict the stability of the InAs film on the GaAs substrate, and answer the question whether diffusion is energetically favorable.

## II. Theory

First, the lattice parameters and the bulk moduli of the GaAs and InAs lattices were determined by calculating the electronic total energy as a function of the lattice parameter. The lattice parameter perpendicular to the interface and the energy of the strained InAs were determined by minimizing the energy of the strained InAs lattice. The elastic constants of GaAs were calculated from the curvature of the total energy with respect to judiciously selected strains. Using the calculated lattice parameters and elastic constants, the formation energy of the defect was then calculated.

In the calculation of the formation energy of a defect, the interactions of the atoms near the defect are beyond the scope of the elastic theory and thus they must be

computed by a more fundamental approach. In this work, the density functional theory in the local density approximation was used. The range of the elastic interactions, however, is too long to be treated by the *ab-initio* method, in which a small number of atoms can be included only. A linear elastic continuum was then used to model the part of the crystal that was not included in the *ab-initio* calculation. By using a combined approach, the formation energy of the defect, including the long-range elastic strain energy, was computed.

The *ab-initio* calculations were performed by the Vienna *Ab-initio* Simulation Package<sup>(5-7)</sup> (VASP), a program based on the local density approximation<sup>(8,9)</sup> of the density functional theory. The crystal is modeled by a periodic replication of a so-called supercell. For a calculation of the energy of a pure infinite lattice, the primitive cell can be used as a supercell, but for calculations of surfaces, interfaces or alloys, larger supercells are needed. Ultrasoft pseudopotentials<sup>(10,11)</sup> describing the interaction between ions and electrons and the Ceperly-Alder exchange-correlation function, as parameterized by Perdew and Zunger<sup>(12)</sup>, were used to construct the Hamiltonians. The Brillouin-zone (BZ) integrations used Monkhorst-Pack<sup>(13)</sup> special k-points. The electronic free energy minimization was done by a matrix-diagonalization routine based on a sequential band-by-band residual minimization method of the one-electron energies<sup>(7,14)</sup>.

The formation energy of the  $\text{In}_{\text{Ga}}$  defect can be defined as

$$E_{\text{form}} = \lim_{n \rightarrow \infty} [E_{\text{InGa}_{n-1}\text{As}_n} - E_{\text{InAs}} - (n-1)E_{\text{GaAs}}] \quad (1)$$

where  $E_{\text{InGa}_{n-1}\text{As}_n}$  is the energy of a supercell consisting of one Indium,  $n-1$  Gallium and  $n$  Arsenic atoms,  $E_{\text{InAs}}$  and  $E_{\text{GaAs}}$  are the energies of unit cells of InAs and GaAs respectively.

The calculation of each term in eq. (1) requires a supercell of different size, and this can lead to various numerical errors, *e.g.* those involving using different sets of k-points. To avoid this problem, we separated the calculation into two parts so that the small energetic differences were computed only for cases where all the energies involved came from supercells with the same size. The lattice parameter and the geometry changes were computed separately using small supercells where a large number of k-points for the BZ integration and a high cut-off energy could be used to reduce the numerical errors. Thus, for computational convenience we defined  $E_{\text{form}}$  as (see Fig. 1),

$$E_{\text{form}} = E_{\text{chem}} + E_{\text{elastic}}, \quad (2)$$

where  $E_{\text{elastic}}$  is defined as the energy necessary for changing the lattice parameter of InAs from its equilibrium value to that of GaAs,

$$E_{\text{elastic}} = E_{\text{InAs}}(a = a_{\text{GaAs}}) - E_{\text{InAs}}(a = a_{\text{InAs}}). \quad (3)$$

$E_{\text{InAs}}(a = a_{\text{GaAs}})$  and  $E_{\text{InAs}}(a = a_{\text{InAs}})$  are the energies of InAs at the GaAs lattice parameter and at its own

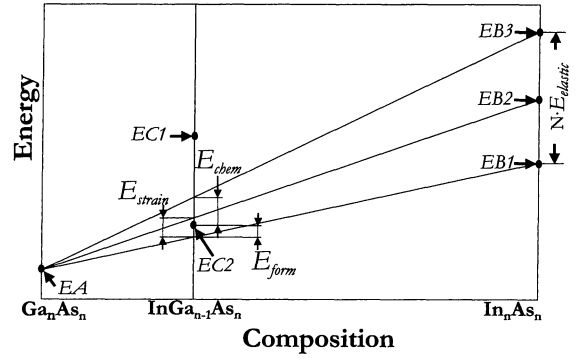


Fig. 1 Schematic diagram of energy versus composition of the  $\text{In}_m \text{Ga}_{n-m} \text{As}_n$  supercell.  $EA$  is the energy of the cubic GaAs with the lattice parameter  $a = a_{\text{GaAs}}$ .  $EB1$ ,  $EB2$ , and  $EB3$  are the energies of cubic InAs with  $a = a_{\text{InAs}}$ , strained tetragonal InAs with  $a = a_{\text{GaAs}}$  and  $c$  optimized, and cubic InAs with  $a = a_{\text{GaAs}}$ , respectively. The strain energy of the tetragonal InAs  $E_{\text{strain}}$  equals  $EB2/n$ .  $EC1$  and  $EC2$  are the energies of the  $\text{InGa}_{n-1}\text{As}_n$  supercell calculated with  $a = a_{\text{GaAs}}$ , without and with atomic relaxation.  $E_{\text{form}}$ ,  $E_{\text{elastic}}$  and  $E_{\text{chem}}$  were defined in eq. (2), eq. (3) and eq. (4), respectively. Note that for clarity the energies and compositions are not plotted to scale.

equilibrium lattice parameter, respectively.  $E_{\text{chem}}$  is simply the energy required for mixing the two materials, and is defined as

$$E_{\text{chem}} = E_{\text{InGa}_{n-1}\text{As}_n}(a = a_{\text{GaAs}}) - \frac{1}{n} E_{\text{In}_n\text{As}_n}(a = a_{\text{GaAs}}) - \frac{n-1}{n} E_{\text{Ga}_n\text{As}_n}(a = a_{\text{GaAs}}), \quad (4)$$

where  $E_{\text{InGa}_{n-1}\text{As}_n}$ ,  $E_{\text{In}_n\text{As}_n}$  and  $E_{\text{Ga}_n\text{As}_n}$  denote the energy of supercells of  $\text{InGa}_{n-1}\text{As}_n$ ,  $\text{In}_n\text{As}_n$  and  $\text{Ga}_n\text{As}_n$ , respectively. Note that these supercells all have the GaAs lattice parameter and that the atomic positions of the  $\text{InGa}_{n-1}\text{As}_n$  supercell are optimized by minimizing the energy.

In eq. (4),  $E_{\text{chem}}$  is to be calculated in a supercell of  $\text{InGa}_{n-1}\text{As}_n$  with a fixed volume  $V_0$  corresponding to the volume of  $\text{Ga}_n\text{As}_n$ . The formation energy in eq. (2) then, based on the assumption that the chemical interactions between the defect and the host lattice is completely confined within the supercell. While it is true that chemical interactions and irregular atomic relaxations are normally limited to the immediate vicinity of the defect, a smoothly decaying elastic interaction is expected over a longer range. To account for this, the supercell is thought of as being embedded in an infinite GaAs crystal, and the cell volume is allowed to change. This volume change causes a change in the supercell energy  $\Delta E_{\text{cell}}$  and the strain energy  $\Delta E_{\text{con}}$  of the crystal that it is embedded in. The total energy change  $\Delta E_{\text{long}}$  then, is given by

$$\Delta E_{\text{long}}(V) = \Delta E_{\text{cell}}(V) + \Delta E_{\text{con}}(V),$$

where

$$\Delta E_{\text{cell}}(V) = E_{\text{InGa}_{n-1}\text{As}_n}(V) - E_{\text{InGa}_{n-1}\text{As}_n}(V_0). \quad (6)$$

The strain energy  $\Delta E_{\text{con}}(V)$  can be calculated within a continuum approximation most simply when the supercell is a sphere and the material is isotropic. In this case, the expansion of the supercell causes a spherical displacement field in the continuum which depends on the distance  $r$  to the defect only. The general form<sup>(15)</sup> of the displacement field is given as,

$$u(r) = Ar + Br^{-2}. \quad (7)$$

The constants  $A$  and  $B$  are determined by the boundary conditions for  $u(r)$  at the supercell radius  $R_0$  and  $r = \infty$ .  $\Delta E_{\text{con}}$  is given by

$$\Delta E_{\text{con}} = 16\pi\mu R(R - R_0)^2, \quad (8)$$

where  $R_0$  and  $R$  are the radius of the supercell before and after expansion, and  $\mu$  is the Lamé coefficient.

However, a spherical supercell can not fill the 3D space and thus strictly speaking cannot be used. In our calculation the defects were distributed in an fcc structure, so the Wigner-Seitz cell of the defect was a regular rhombic dodecahedron, which approximates a sphere. The isotropic assumption is not quite true for GaAs, so we took an average value for the Lamé elastic constant  $\mu$ ,

$$\mu = \frac{1}{2}(\mu_1 + \mu_2), \quad \mu_1 = C_{44}, \quad \mu_2 = \frac{1}{2}(C_{11} - C_{12}). \quad (9)$$

The equilibrium volume of the supercell (see Fig. 2) is determined by minimizing the total change of the energy  $\Delta E_{\text{long}}(V)$ . The formation energy of the defect then, is given by

$$E_{\text{form}} = E_{\text{chem}} + E_{\text{elastic}} + \min_V [\Delta E_{\text{long}}(V)] \quad (10)$$

As computing resources are limited, and as numerical errors overwhelm  $E_{\text{form}}$  as  $n$  is increased, eq. (1) is normally approximated by choosing  $n$  between 10–100. In this work,  $n=27$  was chosen, and supercells containing up to 54 atoms with volumes of  $(3a_0)^3/4$  were used.

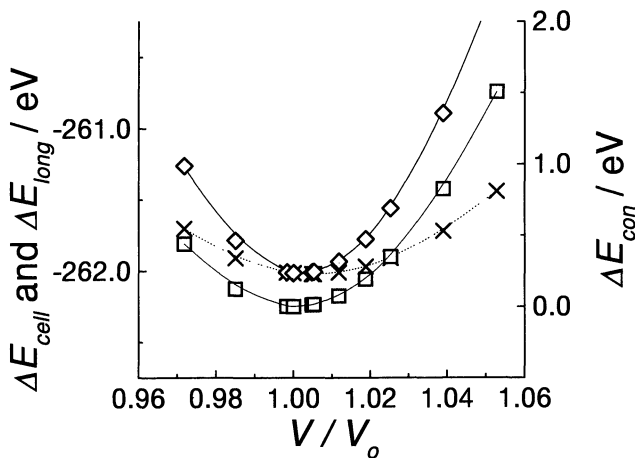


Fig. 2 Energy of the  $\text{InGa}_{n-1}\text{As}_n$  supercell ( $n=27$ )  $\Delta E_{\text{cell}}$  ( $\times$ ), strain energy  $\Delta E_{\text{con}}$  ( $\square$ ), and total energy  $\Delta E_{\text{long}} = \Delta E_{\text{cell}} + \Delta E_{\text{con}}$  ( $\diamond$ ) as a function of the supercell volume. Note that the plot of  $\Delta E_{\text{con}}$  was shifted, but has the same scale as  $\Delta E_{\text{cell}}$  and  $\Delta E_{\text{long}}$ .

Table 1 Calculated and experimental values of lattice parameters  $a_0$  and bulk moduli  $B_0$  of GaAs and InAs.

Material	Calculated values		Experimental values	
	$a_0$ (nm)	$B_0$ (GPa)	$a_0$ (nm)	$B_0$ (GPa)
GaAs	0.5603	75.0	0.56440	75.4
InAs	0.6018	59.9	0.60498	60.0

Note: Experimental values of bulk moduli are from Ref. (16). Experimental values of lattice parameters are from Ref. (17), and have been extrapolated from 300 K to 0 K using the room temperature linear thermal expansion coefficient.

### III. Results

#### 1. Lattice parameters and bulk moduli

The energies of the fcc GaAs and InAs lattices have been computed as a function of the lattice parameter, from 0.535 to 0.595 nm for GaAs and from 0.550 to 0.650 nm for InAs. The calculations were performed using the primitive unit cells with a cut-off energy of 144 eV, and 8,000 plane-waves were used to expand the wavefunction. The BZ integrations were performed in the irreducible part using 165 k-points. The calculated energies were fitted to Birch form,

$$E(V) = E_0 + \frac{9}{8} B_0 V_0 \left[ \left( \frac{V_0}{V} \right)^{2/3} - 1 \right]^2 + \frac{9}{16} B_0 V_0 (B'_0 - 4) \left[ \left( \frac{V_0}{V} \right)^{2/3} - 1 \right]^3 + \sum_{n=4}^N \gamma_n \left[ \left( \frac{V_0}{V} \right)^{2/3} - 1 \right]^n, \quad (11)$$

where  $E$  and  $V$  are the energy and volume, the subscript  $0$  indicates an equilibrium value, and  $B_0$  and  $B'_0$  are the bulk modulus and its derivative with respect to the pressure, respectively. The result is shown in Table 1.

#### 2. Strained InAs

The coherent layer of InAs was modeled by a strained InAs lattice. The interface was assumed to be the (100) plane, and the lattice parameter in the interface plane was assumed to be equal to that of GaAs. This assumption is justified for the first few monolayers of InAs. The lattice parameter in the [100] direction was determined by minimizing the energy. The calculations were done using a tetragonal unit cell with two formula units (f.u.) of InAs. The cut-off energy was set to 144 eV and 8,000 plane-waves were used to expand the wavefunction. The BZ integrations were performed in the irreducible part using 196 k-points. The strained lattice was found to have a lattice parameter in the perpendicular direction of 0.6472 nm, giving a  $c/a$  of 1.155. Tetragonal InAs is 173 meV/f.u. (16.7 kJ/mol) higher in energy than the equilibrium lattice.

#### 3. Elastic constants of GaAs

The elastic constants  $C_{ij}$  were calculated following a

method outlined in Ref. (18).  $C_{11}$ ,  $C_{12}$ , and  $C_{44}$  were calculated from the curvature of the total energy with respect to the strain, and from the bulk modulus. Volume conserving orthorhombic and monoclinic strains were used in which the Taylor expansion of the strain energy contains second, fourth and higher powers of the strain only. The absence of third order terms in the strain makes determination of the curvature more accurate<sup>(18)</sup>. Primitive unit cells were used, the cut-off energy was set to 144 eV, and the wavefunctions were expanded with 8,000 plane-waves. Integrations in the irreducible section of the BZ used 125 k-points. Two set of calculations were performed—one with the lattice parameter set to the calculated value of 0.5603 nm and the other with the experimental value of 0.5653 nm. The calculated and the experimental elastic constants are shown in **Table 2**. The table shows that the calculated  $C_{11}$  and  $C_{12}$  agree well

with experiment, but the calculated  $C_{44}$  differs appreciably from the experimental data. The agreement between calculation and experiment is better for the calculation based on the experimental lattice parameter. This implies that a significant part of the error of the calculation of the elastic constants came from the error of the calculation of the lattice parameter. For the sake of consistency, in the following calculations we used the elastic constants calculated at the calculated lattice parameter.

#### 4. Formation energy of In<sub>Ga</sub> defect

In the *ab-initio* part of the formation energy calculation,  $E_{\text{elastic}}$  was calculated with the unit cell of InAs, a cut-off energy of 200 eV and 8000 plane-waves. The BZ integrations were performed using 286 k-points in the irreducible part. For the calculation of  $E_{\text{chem}}$  and  $E_{\text{cell}}$ , the supercells consisted of 27 cations and 27 anions (As), a cut-off energy of 200 eV and 76233 plane-waves were used, and the BZ integrations were done using 10 k-points in the irreducible part. The atomic positions in the In<sub>27</sub>As<sub>27</sub> and Ga<sub>27</sub>As<sub>27</sub> supercells were set according to the usual Sphalerite structure. The atomic positions of the InGa<sub>26</sub>As<sub>27</sub> supercell were initialized according to the Sphalerite-type GaAs structure, and were subsequently optimized by a conjugate-gradient minimization of the total energy. The optimized supercell was found to have an energy 0.375 eV below that of the unoptimized su-

Table 2 Calculated and experimental values of elastic constants of GaAs.

Elastic Constant (GPa)	Calculation		Experiment
	$a=0.5603$ nm	$a=0.5653$ nm	$a=0.5653$ nm
$C_{11}$	115.9	118.6	118.77
$C_{12}$	54.6	53.2	53.72
$C_{44}$	80.6	73.7	59.44

Note: Experimental values are from Ref. (16).

Table 3 Relaxation of the 53 atoms around an In<sub>Ga</sub> defect in an InGa<sub>26</sub>As<sub>27</sub> supercell. The atoms are grouped according to their initial relative distances from the defect into 7 shells. The supercell is a rhombic dodecahedron with the defect at the center.

Shell	Distance (nm)	Atomic species	No. of atoms	Initial relative position ( $a_0$ )	Relaxation ( $a_0$ )	Constraints
1	0.2426	As	1	$\frac{1}{4}$ [111]	0.01251 [111]	
			3	$\frac{1}{4}$ $\langle 1\bar{1}\bar{1} \rangle$	0.01251 $\langle 1\bar{1}\bar{1} \rangle$	
2	0.3962	Ga	3	$\frac{1}{2}$ $\langle 011 \rangle$	$2.8 \times 10^{-4}$ $\langle 1\bar{1}\bar{1} \rangle$	
			3	$\frac{1}{2}$ $\langle 0\bar{1}\bar{1} \rangle$	$2.8 \times 10^{-4}$ $\langle \bar{1}\bar{1}\bar{1} \rangle$	
			6	$\frac{1}{2}$ $\langle 01\bar{1} \rangle$	$2.8 \times 10^{-4}$ $\langle 11\bar{1} \rangle$	
3	0.4646	As	3	$\frac{1}{4}$ $\langle 11\bar{3} \rangle$	$4.8 \times 10^{-5}$ $\langle \bar{1}\bar{1}0 \rangle + 2.0 \times 10^{-5}$ $\langle 00\bar{1} \rangle$	
			3	$\frac{1}{4}$ $\langle \bar{1}\bar{1}\bar{3} \rangle$	$4.8 \times 10^{-5}$ $\langle 110 \rangle + 2.0 \times 10^{-5}$ $\langle 00\bar{1} \rangle$	
			6	$\frac{1}{4}$ $\langle 1\bar{1}\bar{3} \rangle$	$4.8 \times 10^{-5}$ $\langle \bar{1}10 \rangle + 2.0 \times 10^{-5}$ $\langle 001 \rangle$	
4	0.5603	Ga	6	$\pm \langle 001 \rangle$	$\pm 1.2 \times 10^{-4}$ $\langle 001 \rangle$	
5	0.6106	As	3	$\frac{1}{4}$ $\langle 133 \rangle$	$2.2 \times 10^{-4}$ $\langle 100 \rangle$	1
			1	$\frac{1}{4}$ [133]	$2.2 \times 10^{-4}$ [100]	1
			1	$\frac{1}{4}$ [313]	$2.2 \times 10^{-4}$ [100]	1
			1	$\frac{1}{4}$ [331]	$2.2 \times 10^{-4}$ [100]	1
			1	$\frac{1}{2}$ [112]	$5.0 \times 10^{-5}$ [111]	2
6	0.6862	Ga	1	$\frac{1}{2}$ [112]	$5.0 \times 10^{-5}$ [111]	2
			1	$\frac{1}{2}$ [121]	$5.0 \times 10^{-5}$ [111]	2
			1	$\frac{1}{2}$ [112]	$5.0 \times 10^{-5}$ [111]	2
			1	$\frac{1}{2}$ [112]	$5.0 \times 10^{-5}$ [111]	2
			1	$\frac{1}{2}$ [112]	$8.3 \times 10^{-6}$ [111]	2
			1	$\frac{1}{2}$ [112]	$8.3 \times 10^{-6}$ [111]	2
			1	$\frac{1}{2}$ [112]	$8.3 \times 10^{-6}$ [111]	2
			1	$\frac{1}{2}$ [112]	$8.3 \times 10^{-6}$ [111]	2
			1	$\frac{1}{2}$ [121]	$8.3 \times 10^{-6}$ [111]	2
			1	$\frac{1}{2}$ [121]	$8.3 \times 10^{-6}$ [111]	2
7	0.7279	As	1	$\frac{1}{4}$ [115]	$5.5 \times 10^{-5}$ [111]	2
			1	$\frac{1}{4}$ [115]	$5.5 \times 10^{-5}$ [111]	2
			1	$\frac{1}{4}$ [115]	$5.5 \times 10^{-5}$ [111]	2
			1	$\frac{1}{4}$ [151]	$5.5 \times 10^{-5}$ [111]	2
			1	$\frac{3}{4}$ [111]	[000]	3

Note: In this table the symbol  $\langle 112 \rangle$  means all of the following directions [112], [121], and [211]. The number in the last column shows the number of symmetry planes which intersect the atomic position. The symmetry planes artificially restricted the atomic relaxation.

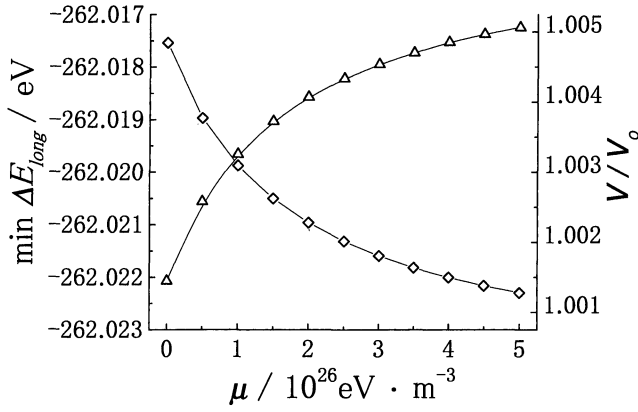


Fig. 3 Minimum of the total energy  $\Delta E_{\text{long}}$  ( $\Delta$ ) and the corresponding  $V/V_0$  ( $\diamond$ ) as a function of the Lamé constant  $\mu$ .

percell. The atomic relaxations are shown in Table 3. The relaxation of atoms from their initial positions decayed rapidly with the distance from the defect. Most of the relaxation occurred in the nearest-neighbor shell. Note that the atoms on the 5<sup>th</sup> to 7<sup>th</sup> shells were on the boundary of the supercell, and therefore were shared among the adjacent supercells. The numbers of atoms shown in the table has been divided with the appropriate factors.  $E_{\text{elastic}}$  was found to be 0.550 eV and  $E_{\text{chem}}$  was  $-0.380$  eV, thus the formation energy  $E_{\text{form}}$  of the defect was 0.170 eV ( $2.72 \times 10^{-20}$  J). The minimum value of  $E_{\text{cell}}(V)$  was found at the volume corresponding to  $\Delta V/V_0 = 4.85 \times 10^{-3}$ , and the energy was lower than that of the unexpanded supercell by 7 meV.

Using the values of the elastic constants calculated in Section III.3 the elastic energy of the continuum outside the supercell was calculated as a function of the supercell volume. The total reduction in the energy  $\Delta E_{\text{long}}(V)$  was found to have a minimum at the volume corresponding to  $\Delta V/V_0 = 1.67 \times 10^{-3}$ , and the energy was lower than that of the unexpanded supercell by 3 meV. As we have shown in Section III.3, there is an appreciable uncertainty in the calculated value of  $C_{44}$ , and thus in the value of  $\mu$ . Our calculated value of  $\mu$  is  $3.47 \times 10^{26}$  eV/m<sup>3</sup>, and the experimental value is  $2.8 \times 10^{26}$  eV/m<sup>3</sup>. Fortunately, the value of  $\mu$  is in the range that the minimum  $\Delta E_{\text{long}}$  is not very sensitive to it—the minimum  $\Delta E_{\text{long}}$  varies by 0.5 meV when  $\mu$  varies between 3 to  $4 \times 10^{26}$  eV/m<sup>3</sup> (see Fig. 3). The volume relaxation contributes  $-3$  meV to the formation energy of the defect, and the formation energy of the In<sub>Ga</sub> defect in GaAs is 0.167 eV.

The defect formation energy was in reasonable agreement with the result, 0.197 eV, extracted from the work by J. Y. Shen *et al.*<sup>(19)</sup>, where the interaction parameters for the pseudobinary solid were obtained from a thermodynamic assessment of the As–Ga–In ternary system. Assuming that the energy of mixing of the InAs–GaAs solid solution can be represented by a nearest-neighbor effective pair interaction between cation atoms only, the In<sub>Ga</sub> defect energy completely determines the configurational thermodynamics<sup>(20)</sup>. Using the In<sub>Ga</sub> defect energy computed in this work, the cluster variation method<sup>(21)</sup> in

the tetrahedron approximation then gives a miscibility gap with a maximum temperature of 546°C. This is in perfect agreement with the temperature of 533°C reported in the assessment<sup>(19)</sup>. At room temperature, InAs was computed to have a very low solubility in GaAs of just 0.15 at%.

For the InAs/GaAs heterostructure, however, the strain raises the energy and the solubility of InAs. As shown in Sect. III.2, in the case of the coherent epitaxial InAs consisting of just a few monolayers, the strain energy is 0.173 eV/f.u., greater than the formation energy of In<sub>Ga</sub> (shown as  $E_{\text{strain}}$  and  $E_{\text{form}}$ , respectively, in Fig. 1), thus in this case the solution energy is negative and such layers are not thermodynamically stable with respect to a dilute solid solution. A small coherent InAs precipitate in GaAs has an even higher strain energy ( $E_{\text{elastic}} = 0.550$  eV/f.u.), and hence can not exist in equilibrium either.

#### IV. Conclusion

The local density approximation of the density functional theory has been applied to the calculation of a few fundamental properties of GaAs and InAs crystals with satisfactory results. Only in the calculation of  $C_{44}$  of GaAs did a significant difference with experimental data occur. The difference could in part be attributed to the error in the calculated equilibrium lattice parameter. The formation energy of In<sub>Ga</sub> was calculated, and the volume relaxation and the elastic strain energy of the crystal outside the supercell contributed only a small correction to the formation energy. From the defect formation energy the maximum temperature of the miscibility gap of InAs–GaAs was determined, and the result was in good agreement with the result of a thermodynamic assessment<sup>(19)</sup> of the As–Ga–In ternary system. Coherent precipitates of InAs in GaAs and coherent InAs layers consisting of a few monolayers on the (100) surface of GaAs were predicted to be thermodynamically unstable with respect to a dilute solid solution.

#### REFERENCES

- (1) F. Houzay, C. Guille, J. M. Moison, P. Henoc and F. Barthe: *J. Cryst. Growth*, **81** (1987), 67–72.
- (2) S. Guha, A. Maduhkar and K. C. Rajkumar: *Appl. Phys. Lett.*, **57** (1990), 2110–2112.
- (3) C. W. Snyder, B. G. Orr, D. Kessler and L. M. Sander: *Phys. Rev. Lett.*, **66** (1991), 3032–3035.
- (4) P. B. Joyce, T. J. Krzyzewski, G. R. Bell, B. A. Joyce and T. Jones: *Phys. Rev. B*, **58** (1998), R15981–R15984.
- (5) G. Kresse and J. Hafner: *Phys. Rev. B*, **47** (1993), 558–561.
- (6) G. Kresse and J. Furthmüller: *Phys. Rev. B*, **54** (1996), 11169–11185.
- (7) G. Kresse and J. Furthmüller: *Comp. Mat. Sci.*, **6** (1996), 15–50.
- (8) P. Hohenberg and W. Kohn: *Phys. Rev.*, **136** (1964), B864–B871; W. Kohn and L. J. Sham: *Phys. Rev.*, **140** (1965), A1133–A1138.
- (9) R. O. Jones and O. Gunnarsson: *Rev. Mod. Phys.*, **61** (1989), 689–746.
- (10) D. Vanderbilt: *Phys. Rev. B*, **41** (1990), 7892–7895.
- (11) G. Kresse and J. Hafner: *J. Phys.: Condens. Matt.*, **6** (1994), 8245–8257.
- (12) J. P. Perdew and A. Zunger: *Phys. Rev. B*, **23** (1981), 5048–5079.

- (13) H. J. Monkhorst and J. D. Pack: *Phys. Rev. B*, **13** (1976), 5188–5192.
- (14) D. M. Wood and A. Zunger: *J. Phys. A*, **18** (1985), 1343–1359.
- (15) L. D. Landau and E. M. Lifshitz: *Course of Theoretical Physics, Vol. 7, Theory of Elasticity*, 2nd ed., chapter 7, problem 2, Pergamon Press, New York, (1970), pp. 20–21.
- (16) H. J. McSkimin *et al.*: *J. Appl. Phys.*, **38** (1967), 2362–2364.
- (17) *CRC Handbook of Chemistry and Physics*, Ed. D. R. Lide, 79<sup>th</sup> ed. (1998), p. 12–94.
- (18) M. J. Mehl, B. M. Klein and D. A. Papaconstantopoulos: in *Intermetallic Compounds, Principles and Practice*, Vol. 1, Ed. J. H. Westbrook and R. L. Fleischer, Wiley, New York, (1995), Chap. 9, pp. 195–202.
- (19) J. Y. Shen, C. Chatillon, I. Ansara, A. Watson, B. Rugg and T. Chart: *Calphad*, **19** (1995), 215–226.
- (20) Usually, the energy of mixing of a binary system is well represented by a parabola in the composition. Since a parabola is fully determined by 3 parameters, where two of these parameters are already fixed by the requirement that the energy of mixing vanishes for pure components. The single free parameter that remains is fixed by the solution energy (which is the slope of the energy of mixing at low concentration limit). Thus, the calculated InAs–GaAs solution energy determines completely the energy of mixing. When the energy of mixing is a parabola, it can be shown that the interactions are of a pairwise type only. Assuming then, that only the nearest neighbor effective pair interaction matters, an effective nearest neighbor pair interaction can be extracted from the energy of mixing.
- (21) D. de Fontaine: in *Solid State Physics*, ed. by H. Ehrenreich, F. Seitz and D. Turnbull, Academic Press, New York, vol. **34** (1979), pp. 73–274.